HHS Public Access

Author manuscript

Chem Commun (Camb). Author manuscript; available in PMC 2020 February 05.

Published in final edited form as:

Chem Commun (Camb). 2019 February 05; 55(12): 1829–1832. doi:10.1039/c8cc09729a.

Sterol A-ring plasticity in hedgehog protein cholesterolysis supports a primitive substrate selectivity mechanism

Daniel A. Ciulla[A], **Andrew G. Wagner**[a], **Liu Xinyue**[D], **Courtney L. Cooper**[A], **Michael T. Jorgensen**[B], **Chunyu Wang**[D], **Puja Goyal**[A], **Nilesh K. Banavali**[C,*], **John Pezzullo**[B], **José-Luis Giner**[B,*], and **Brian P. Callahan**[A,*]

[a]Chemistry Department, Binghamton University, Binghamton, New York 13902, USA.

[b]Department of Chemistry, SUNY-ESF, Syracuse, New York 13210, USA.

[c]NYS Department of Health, ESP C419B, Biggs Laboratory, Wadsworth Center, Empire State Plaza, Albany, New York 12201-0509, USA.

[d]Biology Department, Rensselaer Polytechnic Institute, 110 8th Street, Troy, NY 12180, USA.

Abstract

Cholesterolysis of Hedgehog family proteins couples endoproteolysis to protein C-terminal sterylation. The transformation is self-catalyzed by HhC, a partially characterized enzymatic domain found in precursor forms of Hedgehog. Here we explore spatial ambiguity in sterol recognition by HhC, using a trio of derivatives where the sterol A-ring is contracted, fused, or distorted. Sterylation assays indicate that these geometric variants react as substrates with relative activity: cholesterol, 1.000> A-ring contracted, 0.100> A-ring fused, 0.020> A-ring distorted, 0.005. Experimental results and computational sterol docking into the first HhC homology model suggest a partially unstructured binding site with substrate recognition governed in large part by hydrophobic interactions.

Graphical Abstract

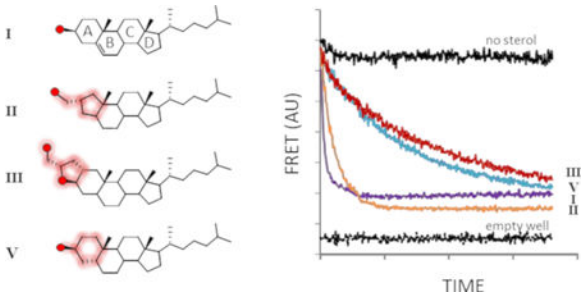

* callahan@binghamton.edu. * jlginer@esf.edu. * nilesh.banavali@health.ny.gov.

Electronic Supplementary Information (ESI) available: [details of any supplementary information available should be included here]. See DOI: 10.1039/x0xx00000x

Conflicts of interest

There are no conflicts to declare.

Proteins in the Hedgehog (Hh) family undergo a self-catalyzed endoproteolytic event called cholesterolysis in which the nucleophilic agent is cholesterol. Cholesterolysis separates precursor Hh into two polypeptides: a sterylated fragment with cell-signaling activity (HhN-sterol), and a partially characterized enzymatic fragment, abbreviated HhC (Fig. 1A). The entire transformation appears to be brought about by HhC through an acyl relay mechanism analogous to self-splicing inteins[1]. However, the specific interactions involved in cholesterol recruitment and activation by HhC remain largely unresolved. Thus we have a limited biochemical understanding of how congenital mutations in HhC pose risk factors for severe birth defects[2]; while dysregulated Hh expression promotes the progression of sporadic tumors[3].

Cholesterol is not the only substrate accepted by HhC. In *Drosophila melanogaster*, which lacks the full complement of genes for cholesterol biosynthesis, the native substrate for HhC may be a dietary sterol such as yeast ergosterol[4, 5]. In humans with the congenital disorder Smith-Lemli-Opitz syndrome (SLOS), cholesterol is likely replaced to some extent by the metabolic precursor, 7-dehydro-cholesterol[6]. Abiraterone is a synthetic anti-androgen used to treat advanced prostate cancer through inhibition of cytochrome P450-17A1[7, 8]. We reported that abiraterone exhibits robust substrate activity with HhC[9]. Other synthetic variants bearing modifications to cholesterol's isooctyl tail also show substrate activity and have been useful for metabolic labeling [10]. Together, these studies indicate that the substrate tolerance of HhC is relatively broad, at least toward sterols with alterations distant from the site of bond scission.

Here, geometric tolerance is probed at the reaction center using cholesterol A-ring analogs. The A-ring contains sterol's nucleophilic substituent and is therefore expected to be under stringent constraints. We investigate the substrate activity of an A-ring contracted sterol (**II**), a pentacyclic cholesterol derivative (**III**), and the nonplanar cholesterol analogue, coprostanol (**V**) (Fig. 1B). We employ a continuous assay to monitor HhC activity in the presence of potential substrates by changes in FRET[11, 12]. The assay uses a 3-part Hh fusion construct, C-H-Y, where HhC is flanked by cyan fluorescent protein and yellow fluorescent protein (Fig. 2A). In the presence of substrate, FRET signal between CFP and YFP rapidly diminishes with release of sterylated CFP. SDS-PAGE, RP-HPLC and mass spectrometry provide independent means of confirming protein sterylation[9, 11, 13].

We first tested *A*-nor cholestanol (**II**), a contracted analogue with a cyclopentyl A-ring and hydroxymethyl substituent at the 2-position. The freely rotating primary alcohol of **II** replaces cholesterol's ring-constrained secondary alcohol as the lone nucleophilic group. *A*-nor cholestanol was prepared in two steps from cholestanone[14]. Sterol **II** is reminiscent of naturally occurring *A*-nor sterols identified in the extracts of certain marine sponges [15].

Despite structural deviation from cholesterol, *A*-nor cholestanol displayed robust substrate activity in multiple assays with HhC. Shown in Fig. 2B is the kinetic trace for reaction of 50 μM **II** with the FRET reporter, C-H-Y, where FRET decay reports HhC activity. Controls experiments include reactions with no sterol, with added cholesterol (**I**), and without the C-H-Y construct. Addition of **II** resulted in rapid FRET loss, with $t_{1/2}$ of ~8 min, on par with cholesterol's $t_{1/2}$ value of 3 min. Plots of initial velocity versus substrate concentration

indicated K_m and k_{max} values for **II** that deviated from cholesterol by only ~3-fold (Table 1; Sup. Fig. 1A). To establish sterylation with **II**, we replaced C-H-Y with a closer physiological mimic of Hh precursor, where the human sonic hedgehog signaling domain (SHhN) is translationally fused to *Drosophila* HhC [12]. Addition of substrate sterol activates precursor processing into two products, SHhN-sterol (20 kDa) and DHhC (26 kDa), which readily separate by SDS-PAGE[12]. As displayed in Sup. Fig. 1B, the reaction of SHhN-DHhC with **II** generated the expected products. Further, MALDI-TOF analysis identified the sterylated adduct with **II** (Sup. Table 1). We also assessed the extent of protein sterylation by subjecting the product mixture to reverse-phase HPLC[16]. In Sup. Fig. 2B, control separations are shown of SHhN-DHhC following incubation in the absence and presence of added cholesterol, where peaks are visible for HhN (minor peak, 8.9 min'), and cholesterylated HhN (13.9 min'), respectively. For samples with *A*-nor used as substrate, the putative HhN-**II** product exhibits a retention time (15.1 min') comparable to the cholesterol adduct, consistent with covalent sterylation. Thus, kinetic and product analysis support the notion that at the ground and transition states for protein sterylation, HhC does not strongly discriminate between cyclohexyl and cyclopentyl A-rings nor is there overwhelming preference for secondary over primary alcohol nucleophiles.

We next probed geometric constraints in the opposite sense using an oversized sterol analog in which the A-ring was fused to a hydroxymethyl tetrahydrofuran [17]. Like **II**, sterylation involves attack by an exocyclic primary alcohol. FRET assays of substrate activity indicated that HhC accepted the pentacyclic α epimer (**III**) albeit with modest efficiency. The order of reactivity is apparent from comparison of kinetic traces in Fig. 2B and in steady state kinetic parameters in Table 1, where ground state binding of **III** is 6-fold weaker than cholesterol and the maximum reaction rate is slower by almost 10-fold (see also, Sup. Fig. 1A). Substrate activity of **III** was corroborated by SDS-PAGE analysis using the chimeric Hh precursor, SHhN-DHhC (Sup. Fig. 1B), and by MALDI-TOF (Sup. Table 1). In addition, the HhN product sterylated with pentacyclic sterol **III** exhibited the characteristic extended retention time of 13.4 min' on RP-HPLC (Sup. Fig. 2). Substrate activity with **III** accords in part with the inference above that a ring constrained alcohol is not imperative, while also revealing a reduced degree of promiscuity in accommodating an extra ring. Likewise, the apparent absence of reactivity with the β epimer (**IV**) indicates that the substrate range of HhC is not unlimited. Comparison of 3-D models of **III**, **IV** and cholesterol shows that the –OH group of the unreactive **IV** is displaced relative to cholesterol's –OH group by a distance greater than the –OH group active **III** epimer. If activation of the sterol –OH group involves a distance dependent mechanism like general base catalysis [18, 1920], this could explain the observed stereospecificity.

The last analog we evaluated was coprostanol, 5β-cholestan-3β-OL (**V**), a microbial metabolite of cholesterol [21], which has an A-ring displaced almost 90° (A/B *cis*) compared with the pseudo planar rings of cholesterol (A/B *trans*). Of the A-ring analogs accepted by HhC, coprostanol exhibited the weakest substrate activity. We estimate based on kinetic analysis that the K_m value for **V** is 23 μM and the k_{max} value is 0.27×10^{-3} sec^{-1} (Table 1, and Sup. Fig. 1). Thus, coprostanol binds half as tightly and reacts half as slowly with HhC as pentacyclic sterol **III**. Comparison of coprostanol with cholesterol shows less than 1%

activity. Substrate behavior of coprostanol is supported by SDS-PAGE (Sup. Fig. 1B), MALDI-TOF (Sup. Table 1) and analysis of the product mixture by RP-HPLC, where the reaction generates a late eluting, HhN-coprostanol conjugate (Sup. Fig. 2B). The marginal reactivity of HhC toward coprostanol recalls the specificity observed with sterol sterol sulfotransferases SULT2B1b [22] and glucosylating enzymes [23], which exhibit weak or no activity toward **V**, respectively.

To better understand the substrate ambiguity of HhC, we attempted to integrate the experimental findings with a computational model of HhC-sterol interactions. Early mutagenesis experiments on the *Drosophila melanogaster* HhC suggest a composite structure, where the first 150 amino acids of HhC is a self-splicing module, called HINT, related structurally to inteins [24, 25]; and the final 70 amino acids harbor the sterol binding or recognition region, SRR. While the structural fold of the self-splicing HINT module is well characterized, 3-D structure of the SRR is not yet available. We therefore relied on the published crystal structure of HhC's HINT [25] and sought a homologous scaffold to construct the adjacent sterol binding SRR. By manually performing pair-wise sequence comparisons a SRR scaffold candidate was identified in the small fungal protein cryptogein (PDB ID: 1LRI) [26]. Cryptogein is similar in length to the SRR (90 AA vs. 70 AA) and functions as a sterol binding protein.

Using the cryptogein sequence alignment, we employed MODELLER [27] to generate a provisional homology model of full-length HhC (HINT-SRR) bound to cholesterol. Subsequent optimization through Langevin molecular dynamics (MD) simulations performed using CHARMM program[28] with available CHARMM protein [29] and cholesterol [30] force field parameters positioned cholesterol with its attacking -OH group near to HhC catalytic residues. Additional refinements were undertaken based on HhC sequence conservation (**See Supporting information**).

Docking calculations successfully positioned the A-ring sterol variants at the putative cholesterol binding site in the SRR of the HhC homology model (see overlay Fig. 3). Hydroxyl groups of the sterols also pointed toward the catalytic center, consistent with the proposed mechanism. On the other hand, there was variability among docked positions of sterols in the putative binding site. An obvious molecular explanation for the observed 100-fold range of reactivity among the A-ring variants was not revealed by these initial models. Comparison between the Autodock binding scores and experimental ranking of the sterol analog affinity based on K_m values also did not show full agreement. It is possible that initial sterol-HhC encounter promotes a change in HhC conformation, and that our present modeling does not capture this induced fit. The HhC structure should therefore be considered as a testable hypothesis for the molecular basis of sterol recognition, the first that we are aware of, which is to be improved through further experimental validation and refinement.

Carboxyl terminal sterylation is a defining feature of Hh signaling proteins, with the lipid providing a membrane anchor for cell signaling that is spatially restricted[31]. In the present report, we combined experimental and computational studies of HhC to probe the catalyst's substrate selectivity, expanding on earlier work that established tolerance of HhC toward

sterols bearing modifications of the lipid's isooctyl side chain. The activity observed here of a trio of A-ring cholesterol analogues suggest that the active site of HhC is spatially accommodating even at the reaction center. The nucleophilic substituent can be switched from secondary to primary alcohol; its position altered by contracting the A-ring or installing an extra ring, or by swapping the A-ring configuration, all while retaining activity. We find these observations consistent with the notion that sterol binding by HhC is governed in large part through a primitive selectivity mechanism. Hydrophobic binding, where nonpolar HhC residues simply collapse around the aliphatic substrate through dispersion forces, offers one possibility. This hypothesis would accord with modeling that suggests hydropathic segments of the sterol binding site lack defined secondary structure.

Supplementary Material

Refer to Web version on PubMed Central for supplementary material.

Acknowledgements

We acknowledge generous support from the National Cancer Institute (Grant R01 CA206592) and Department of Defense (Grant W81XWH-14-1-0155). We also acknowledge the upgrade of the 600 MHz NMR spectrometer at SUNY-ESF under NSF grant CHE-1048516 and NIH grant S10 OD012254. This work used the Extreme Science and Engineering Discovery Environment (XSEDE), supported by National Science Foundation grant number ACI-1548562.

Notes and references

1. Porter JA, Young KE and Beachy PA, Science, 1996, 274, 255–259. [PubMed: 8824192]
2. Roessler E, Belloni E, Gaudenz K, Vargas F, Scherer SW, Tsui LC and Muenke M, Hum. Mol. Genet, 1997, 6, 1847–1853. [PubMed: 9302262]
3. Owens AE, de Paola I, Hansen WA, Liu YW, Khare SD and Fasan R, J. Am. Chem. Soc, 2017, 139, 12559–12568. [PubMed: 28759213]
4. Karpen HE, Bukowski JT, Hughes T, Gratton JP, Sessa WC and Gailani MR, J Biol Chem, 2001, 276, 19503–19511. [PubMed: 11278759]
5. Mann RK and Beachy PA, Annu. Rev. Biochem, 2004, 73, 891–923. [PubMed: 15189162]
6. Cooper MK, Wassif CA, Krakowiak PA, Taipale J, Gong R, Kelley RI, Porter FD and Beachy PA, Nat. Genet, 2003, 33, 508–513. [PubMed: 12652302]
7. Attard G, Reid AH, Yap TA, Raynaud F, Dowsett M, Settatree S, Barrett M, Parker C, Martins V, Folkerd E, Clark J, Cooper CS, Kaye SB, Dearnaley D, Lee G and de Bono JS, J Clin. Oncol, 2008, 26, 4563–4571. [PubMed: 18645193]
8. DeVore NM and Scott EE, Nature, 2012, 482, 116–119. [PubMed: 22266943]
9. Bordeau BM, Ciulla DA and Callahan BP, ChemMedChem, 2016, 11, 1983–1986. [PubMed: 27435344]
10. Ciepla P, Magee AI and Tate EW, Biochem. Soc. Trans, 2015, 43, 262–267. [PubMed: 25849927]
11. Owen TS, Ngoje G, Lageman TJ, Bordeau BM, Belfort M and Callahan BP, Anal. Biochem, 2015, 488, 1–5. [PubMed: 26095399]
12. Owen TS, Xie XJ, Laraway B, Ngoje G, Wang C and Callahan BP, Chembiochem, 2015, 16, 55–58. [PubMed: 25418613]
13. Xie J, Owen T, Xia K, Singh AV, Tou E, Li L, Arduini B, Li H, Wan LQ, Callahan B and Wang C, J. Biol. Chem, 2015, 290, 11591–11600. [PubMed: 25787080]
14. Balakrishnan P and Bhattacharyya SC, Indian J. of Chem., Section B: Organic Chemistry Including Medicinal Chemistry, 1986, 25B, 1050–1051.
15. Minale L and Sodano G, J. Chem. Soc., Perkin I 1974 2380–2384.

16. Baker DP, Taylor FR and Pepinsky RB, Methods Mol Biol, 2007, 397, 1–22. [PubMed: 18025709]
17. Giner JL, J. Org. Chem, 2005, 70, 721–724. [PubMed: 15651829]
18. Xie J, Owen T, Xia K, Callahan B and Wang C, J. Am. Chem. Soc, 2016, 138, 10806–10809. [PubMed: 27529645]
19. Ciulla DA, Jorgensen MT, Giner JL and Callahan BP, J. Am. Chem. Soc, 2018, 140, 916–918. [PubMed: 28930454]
20. Schowen KB, Limbach HH, Denisov GS and Schowen RL, Biochim. Biophys. Acta, 2000, 1458, 43–62. [PubMed: 10812024]
21. Garcia JL, Uhia I and Galan B, Microb. Biotechnol, 2012, 5, 679–699. [PubMed: 22309478]
22. Wojciechowski ZA, Zimowski J, Zimowski JG and Lyznik A, Biochim. Biophys. Acta, 1979, 570, 363–370. [PubMed: 497231]
23. Strott CA, Endocr. Rev, 2002, 23, 703–732. [PubMed: 12372849]
24. Xie J, Du Z, Callahan B, Belfort M and Wang C, Biomol. NMR Assign, 2014, 8, 279–281. [PubMed: 23765287]
25. Hall TM, Porter JA, Young KE, Koonin EV, Beachy PA and Leahy DJ, Cell, 1997, 91, 85–97. [PubMed: 9335337]
26. Lascombe MB, Ponchet M, Venard P, Milat ML, Blein JP and Prange T, Acta. Crystallogr. D Biol. Crystallogr, 2002, 58, 1442–1447. [PubMed: 12198300]
27. Webb B and Sali A, Curr. Protoc. Bioinformatics, 2014, 47, 561–5632.
28. Brooks BR, Brooks CL, 3rd, Mackerell AD, Jr., Nilsson L, Petrella RJ, Roux B, Won Y, Archontis G, Bartels C, Boresch S, Caflisch A, Caves L, Cui Q, Dinner AR, Feig M, Fischer S, Gao J, Hodoscek M, Im W, Kuczera K, Lazaridis T, Ma J, Ovchinnikov V, Paci E, Pastor RW, Post CB, Pu JZ, Schaefer M, Tidor B, Venable RM, Woodcock HL, Wu X, Yang W, York DM and Karplus M, J. Comp. Chem, 2009, 30, 1545–1614. [PubMed: 19444816]
29. Best RB, Zhu X, Shim J, Lopes PE, Mittal J, Feig M and Mackerell AD, Jr., J Chem Theory Comput, 2012, 8, 3257–3273. [PubMed: 23341755]
30. Lim JB, Rogaski B and Klauda JB, J. Phys. Chem. B, 2012, 116, 203–210. [PubMed: 22136112]
31. Petrov K, Wierbowski BM and Salic A, Annu. Rev. Cell. Dev. Biol, 2017, 33, 145–168. [PubMed: 28693388]

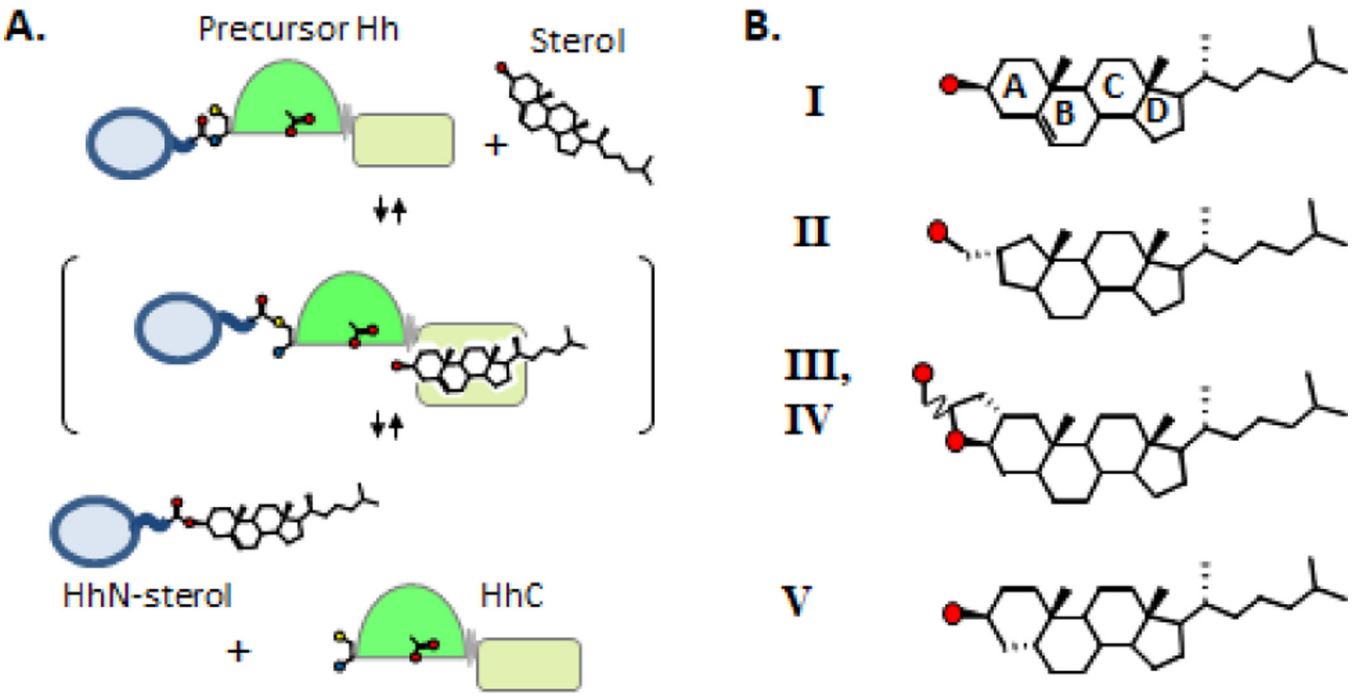

Figure 1.

Assessing A-ring specificity in HhC catalysis. (A) Hedgehog cholesterolysis. Precursor hedgehog undergoes peptide bond rearrangement at a conserved Gly-Cys motif; the resulting thioester is cleaved by substrate sterol (bracket), releasing HhN-sterol and HhC. Catalytic cysteine and aspartate acid residues of HhC depicted as ball-and-strick.(B) Sterols with variant A-ring structures assayed as alternative HhC substrates. Red circles, oxygen atom.

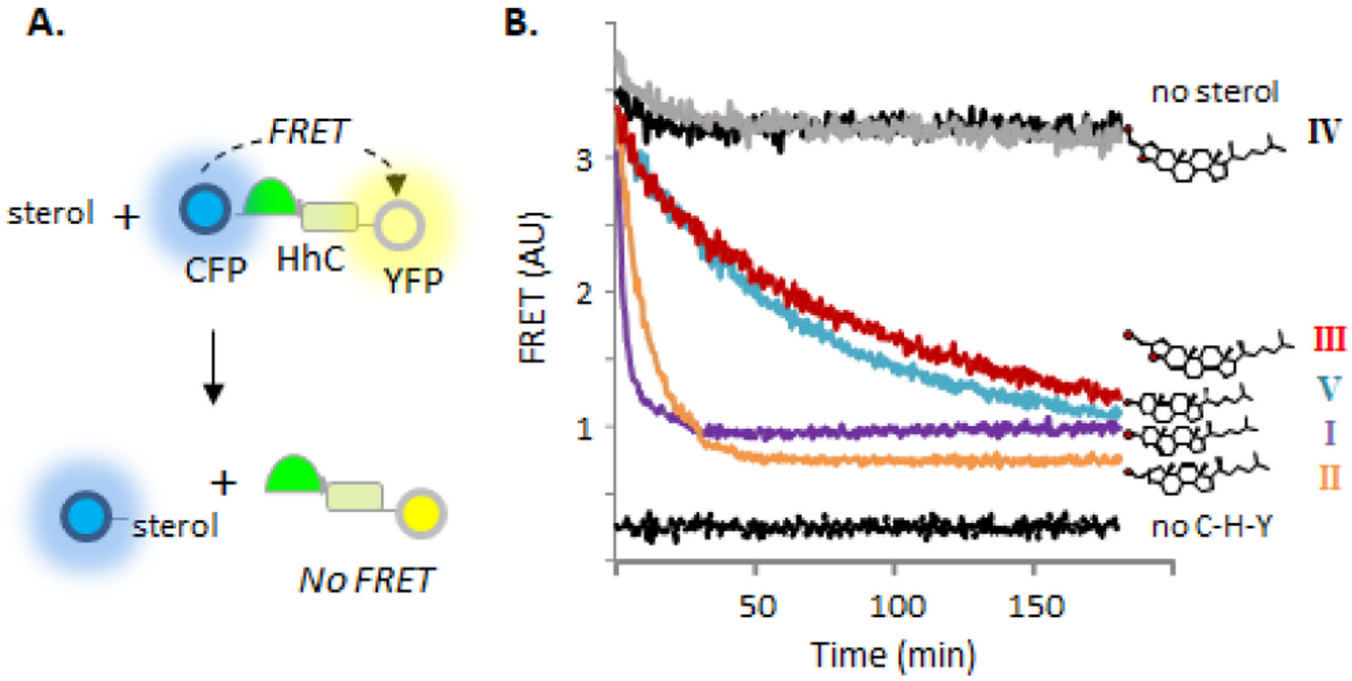

Figure 2.

A-ring derivatives retain substrate activity (A) FRET on/off system for continuous monitoring of HhC activity. A tripartite fusion protein C-H-Y comprises cyan fluorescent protein. Drosophila melanogaster HhC and yellow fluorescent protein; sterolysis separates C-H-Y into C-sterol and H-Y, with FRET signal loss. (B) Sterol A-ring variants exhibit varying substrate activity. Representative kinetic traces for reactions of HhC with the indicated sterols at 50 pM. Control traces with C-H-Y with no sterol (top trace) and wells containing buffer only (bottom trace) in black.

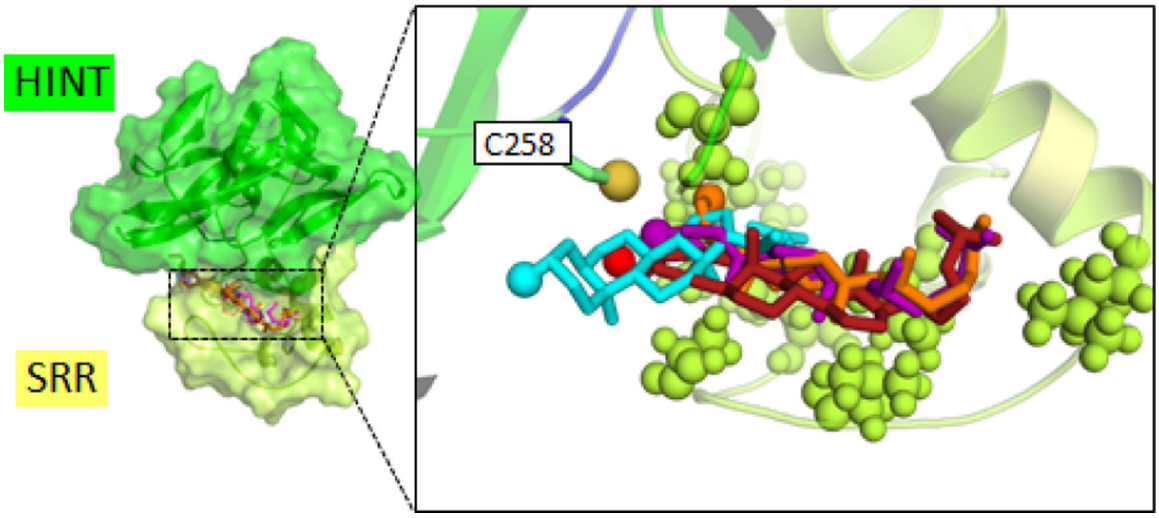

Figure 3.

Computational model of HhC docks sterols near catalytic cysteine residue. Result combines the solved crystal structure of the HINT module (green) with homology model of sterol recognition region (yellow). Sterols positioned using AutoDock. *Right,* expanded view of sterol binding site . Hydrophobic residues of the SRR displayed as spheres. Key catalytic cysteine, C258, residue displayed as sticks with sulfur as sphere. Sterol coloring: cholesterol, orange; II, purple; III, red; V, cyan. Nucleophilic hydroxyl group of each sterol displayed as colored sphere.

Table 1.

Kinetic parameters for sterol substrates with hedgehog HhC using the FRET reporter assay. Standard errors were less than or equal to ±10% for k_{max} values and ±16% for K_M values, n ≥ 3. Relative proficiency compares second order rate constants (k_{max}/K_m).

substrate	k_{max} (s^{-1}) (x10^{-3})	K_M (μM)	*Relative proficiency*
Cholesterol (I)	4.7	1.9	1
II	1.4	4.7	0.1
III	0.49	12	.02
V	0.27	23	.005
IV	<.005	nd	